Physiologia Plantarum
An International Journal for Plant Biology

Physiologia Plantarum 139: 313–323. 2010

Analysis of fast chlorophyll fluorescence rise (O-K-J-I-P) curves in green fruits indicates electron flow limitations at the donor side of PSII and the acceptor sides of both photosystems

Dimitrios Kalachanis and Yiannis Manetas*

Laboratory of Plant Physiology, Department of Biology, University of Patras, Patras GR 265 00, Greece

Correspondence
*Corresponding author,
e-mail: y.manetas@upatras.gr

Received 8 December 2009;
revised 26 January 2010

doi:10.1111/j.1399-3054.2010.01362.x

Limited evidence up to now indicates low linear photosynthetic electron flow and CO_2 assimilation rates in non-foliar chloroplasts. In this investigation, we used chlorophyll fluorescence techniques to locate possible limiting steps in photosystem function in exposed, non-stressed green fruits (both pericarps and seeds) of three species, while corresponding leaves served as controls. Compared with leaves, fruit photosynthesis was characterized by less photon trapping and less quantum yields of electron flow, while the non-photochemical quenching was higher and potentially linked to enhanced carotenoid/chlorophyll ratios. Analysis of fast chlorophyll fluorescence rise curves revealed possible limitations both in the donor (oxygen evolving complex) and the acceptor ($Q_A^- \rightarrow$ intermediate carriers) sides of photosystem II (PSII) indicating innately low PSII photochemical activity. On the other hand, PSI was characterized by faster reduction of its final electron acceptors and their small pool sizes. We argue that the fast reductive saturation of final PSI electron acceptors may divert electrons back to intermediate carriers facilitating a cyclic flow around PSI, while the partial inactivation of linear flow precludes strong reduction of plastoquinone. As such, the photosynthetic attributes of fruit chloroplasts may act to replenish the ATP lost because of hypoxia usually encountered in sink organs with high diffusive resistance to gas exchange.

Introduction

Leaves are optimized for photosynthesis regarding both efficient light capture and diffusion of interfering gases. Yet, chloroplasts may abound also in organs apparently designed for other functions. Thus, flowers, fruits, petioles and stems may be green, and even light remote plant parts such as xylem rays, pith, deeply located seeds and roots may contain some chlorophyll (Aschan and Pfanz 2003, Dima et al. 2006, Pfanz et al. 2002). In bulky, non-foliar and largely heterotrophic organs such as fruits and stems, photosynthesis is believed to assist in the re-assimilation of respiratory CO_2, thus compensating for carbon loss (Bazzaz et al. 1979, Blanke and Lenz 1989, Cernusak and Marshall 2000, Pfanz et al. 2002). Another plausible function is related to the fact that these bulky organs are devoid of stomata or display a low stomatal density. Accordingly, diffusion of gases is hindered and the internal atmosphere becomes extremely enriched in CO_2, while partial pressure of

Abbreviations – ABS, absorbed excitation energy fluxes; DMSO, dimethylsulfoxide; ET, electron transfer; ETR, electron transport rate; PAR, photosynthetically active radiation; PSII, photosystem II; NADPH, nicotinamide adenine dinucleotide phosphate; NPQ, non-photochemical energy quenching; OEC, oxygen evolving complex; RC, reaction centers; RE, reduction of end electron acceptors; SEM, scanning electron microscope; TR, trapped excitation energy flux.

O_2 is very low (Blanke and Lenz 1989, Borisjuk and Rollentschek 2009, Goffman et al. 2004, Pfanz et al. 2002). Hence, photosynthesis may additionally help to avoid acidification because of extremely high CO_2 and alleviate the adverse effects of hypoxia (Borisjuk and Rollentschek 2009, Pfanz et al. 2002). In this sense, photosynthesis in fruits and stems occurs under a specific aerial microenvironment never encountered by leaves. Moreover, the metabolic status of these organs is quite different. Fruits, in particular, and on contrary to leaves, are sinks for both carbon and chemical energy. We argue that the combination of different metabolic needs and the specific constitution of the internal atmosphere in fruits may have shaped the structure and function of photosystems and the associated electron flow. Yet, corresponding reports are scarce.

In some cases, fruit photosynthesis was probed through chlorophyll fluorescence measurements, while leaves were used as controls. Hence, De Lemos Filho and Dos Santos Isaias (2004) and Hetherington et al. (1998) found lower fruit photosystem II (PSII) trapping efficiencies (as F_v/F_m) in *Dalbergia miscolobium and Lycopersicon esculentum*, respectively. Yet, Aschan et al. (2005) reported similar trapping efficiencies in leaves and fruits of *Helleborus viridis*. In all cases, however, the light-adapted PSII yield and corresponding electron linear transport rates displayed considerably lower values in fruits, when compared with leaves. Moreover, Borisjuk et al. (2005) found very low actual PSII yields in light-adapted green soybean seeds. We may, therefore, assume that PSII function and related electron flow activities in chloroplasts of reproductive structures may suffer from considerable limitations, whose nature is still unclear. On this background, we analyzed the polyphasic (O-K-J-I-P) fast chlorophyll fluorescence transients of dark-adapted leaves and pericarps of three species as well as of green seeds in two of the species. Such an analysis takes into account all the intermediate steps of sequential fluorescence increase upon sudden illumination and allows the estimation of partial efficiencies in energy and electron flow along the whole continuum from the initial electron donors of PSII and up to final electron acceptors of PSI (Oukarroum et al. 2009, Strasser et al. 2004, Tsimilli-Michael and Strasser 2008). Accordingly, specific limiting steps can be located.

Materials and methods

Plant material and sampling

Acacia cyanophylla Lindl. (Fabaceae) and *Nerium oleander* L. (Apocynaceae) grown as ornamentals in the Patras University campus and *Ailanthus altissima* (Mill.) Swingle (Simaroubaceae) growing wild in the vicinity were used in this study. Green fruits are produced at late spring (*A. cyanophylla*), early summer (*A. altissima*) and mid-summer to late autumn (*N. oleander*). Sampling was performed at late afternoon of bright days during the last week of May (*A. cyanophylla*), second week of June (*A. altissima*) and first week of September (*N. oleander*). Fruits and corresponding leaves were put in air-tight plastic envelopes internally lined with moistened filter paper and kept all night in the dark at room temperature to be analyzed next morning. Care was taken to harvest south-facing, fully exposed leaves and fruits to avoid confounding effects of light or shade.

Microscopy

Leaf and pericarp stomatal densities were determined on fixed plant material. Leaf and pericarp samples were carefully cut and fixed in 5% glutaraldehyde in phosphate buffer at pH 7 at room temperature for 2 h. Tissue was then post-fixed in 1% OsO_4 at 4°C and dehydrated in a graded acetone series. The dehydrated tissue samples were critical point dried, mounted with a double adhesive tape on stubs, sputter coated with gold and observed with a JEOL 6300 (Japan) scanning electron microscope (SEM). The digitally recorded micrographs were then used to determine the density of stomata, using the *Image Tool 1.25* program (University of Texas Health Science Center, San Antonio, TX).

Pigments

In *A. cyanophylla* and *A. altissima*, discs punched from leaves and pericarps as well as from intact seeds were extracted with mortar and pestle in 100% methanol plus a pinch of $CaCO_3$ and purified sea sand. Hard pericarps from *N. oleander* were difficult to grind; hence the hot dimethylsulfoxide (DMSO) method (Wittman et al. 2001) was used for leaves, pericarps and seeds of this plant. After clearing by centrifugation, the extracts were scanned in a Shimadzu UV-160A double beam spectrophotometer. Pigment concentrations were calculated using the formulae of Lichtenthaler and Wellburn (1983) for methanolic and Wellburn (1994) for DMSO extracts.

Prompt chlorophyll fluorescence measurements in dark-adapted material

Intact leaves, fruits (i.e. pericarps) or seeds (after pericarp removal) were used. All manipulations before fluorescence induction were done under dim light of

less than 0.5 μmol m^{-2} s^{-1}, and samples were kept in the corresponding leaf clips for further 30 min.

Fast chlorophyll fluorescence transients were captured by a Hansatech (Handy-PEA, Hansatech Instruments Ltd, Kings' Lynn, Norfolk, UK) fluorimeter. For excitation, a band of three red (peak at 650 nm) light emitting diodes (LEDs) provided 3000 μmol m^{-2} s^{-1} at sample level and fluorescence recorded from 10 μs to 2 s with data acquisition rate of 10^5, 10^4, 10^3, 10^2 and 10 readings s^{-1} in the time intervals of 10–300 μs, 0.3–3 ms, 3–30 ms and 0.3–2 s, respectively. Cardinal points in the fluorescence vs time curve used for further calculation of biophysical parameters were the following: maximal fluorescence intensity (F_m); fluorescence intensity at 20 μs, considered as the first credible measurement (F_0); fluorescence intensity at 300 μs ($F_{300\ \mu s}$) needed for the calculation of the initial slope (M_0) of the relative variable fluorescence vs time curve; fluorescence intensity at 2 ms and 30 ms, i.e. at the J and I steps, respectively (F_J and F_I). These primary data were used to derive the following parameters according to the JIP-test (Strasser et al. 2004), as extended to analyze also events in or around PSI (Jiang et al. 2008, Tsimilli-Michael and Strasser 2008, Zubek et al. 2009):

(1) The photosynthetic efficiencies at the onset of illumination, i.e. the maximum quantum yield of primary photochemistry $\phi_{Po} = TR_0/ABS = F_v/F_m$ (where TR and ABS denote the trapped and absorbed excitation energy fluxes); the efficiency to conserve trapped excitation energy as redox energy (i.e. electron transfer, ET) $\psi_{Eo} = ET_0/TR_0$; the quantum yield of electron transfer to intermediate electron carriers $\phi_{Eo} = ET_0/ABS = \phi_{Po} \cdot \psi_{Eo}$; the efficiency of electron transfer between intermediate carriers to the reduction of end electron acceptors (RE) of PSI, $\delta_{Ro} = RE_o/ET_0$; and the quantum yield of reduction of end electron acceptors of PSI, $\phi_{Ro} = \phi_{Po} \cdot \psi_{Eo} \cdot \delta_{Ro}$.

(2) The specific fluxes per active (i.e. Q_A-reducing) reaction centers (RC) for absorption (ABS/RC), trapping (TR_0/RC) and dissipation (DI_0/RC).

(3) The relative pool size of the final electron acceptors of PSI [assessed from the upper part of the $(F_t - F_0)/(F_I - F_0)$ transient] and the time needed for half saturation of this pool with electrons donated by intermediate carriers ($t_{1/2}^{(I-P)}$), i.e. the time needed for the fluorescence rise kinetics to reach from the I-step to the half of the I–P distance.

The formulae used to calculate the above parameters are given in the Appendix.

Modulated chlorophyll fluorescence in the light-adapted plant material

Disc of leaves and pericarps, as well as intact seeds were placed in Petri dishes on moistened filter paper. All manipulations were done under dim light of less than 0.5 μmol m^{-2} s^{-1}. An Imaging-PAM system (Walz, Effeltrich, Germany), equipped with blue LEDs providing measuring, actinic and saturation pulse light and a CCD camera for capturing fluorescence was used. The imaging system was not used to exploit heterogeneities in plant material but rather to scan many samples (discs or seeds) simultaneously. Hence, the signal used was that integrated over the whole sample area, avoiding the edges of the discs which were unavoidably wounded by the cork borer. In all cases, the naturally exposed surface of plant material was probed. Before each series of measurements, the instrument probes the sample reflectance in the red (650 nm) and infrared (780 nm) band. A built-in equation is then used for the relative estimation of sample absorptivity as $A = 1 - (R_{650}/R_{780})$, to be used later in the calculation of relative linear electron transport rates. A white filter paper, equally reflecting in the two spectral bands, was used for the system calibration. Following a saturation pulse for the measurement of dark-adapted maximum PSII yield, the sample was illuminated with step-wise increasing actinic irradiances, during which saturation pulses (0.8 s, 2400 μmol m^{-2} s^{-1}) were given every 60 s to close all PSII reaction centers. Duration of each actinic irradiance step was long enough for full photosynthetic induction, typically not less than 5 min. Values of parameters in Fig. 6 were those obtained at the end of each step when fluorescence readings were stable. PSII yield in the dark- or the light-adapted state was computed essentially after Paillotin (1976) as $1 - F_x/F_m$, where F_x is the fluorescence value just before applying a saturating pulse. Hence, dark-adapted PSII yield was computed as $F_v/F_m = (F_m - F_0)/F_m$ (equivalent to ϕ_{Po} measured with the Handy-PEA, see previous section) and light-adapted PSII yield (here designated as ϕ'_{Pt}) as $\Delta F'/F_{m'} = (F_{m'} - F')/F_{m'}$. Non-photochemical energy quenching (NPQ) was computed according to Butler (1978) as $NPQ = (F_m/F_{m'}) - 1 = (F_m - F_{m'})/F_{m'}$. Linear electron transport rate (ETR) was computed as $ETR' = \phi'_{Pt} \cdot PAR \cdot A \cdot 0.5$, where PAR is the incident photosynthetically active radiation, A the computed sample absorptivity and 0.5 a distribution factor assuming equal light absorption by the two photosystems (Genty et al. 1989).

Statistics

Significance of differences in the measured parameters between leaves, pericarps and seeds were assessed

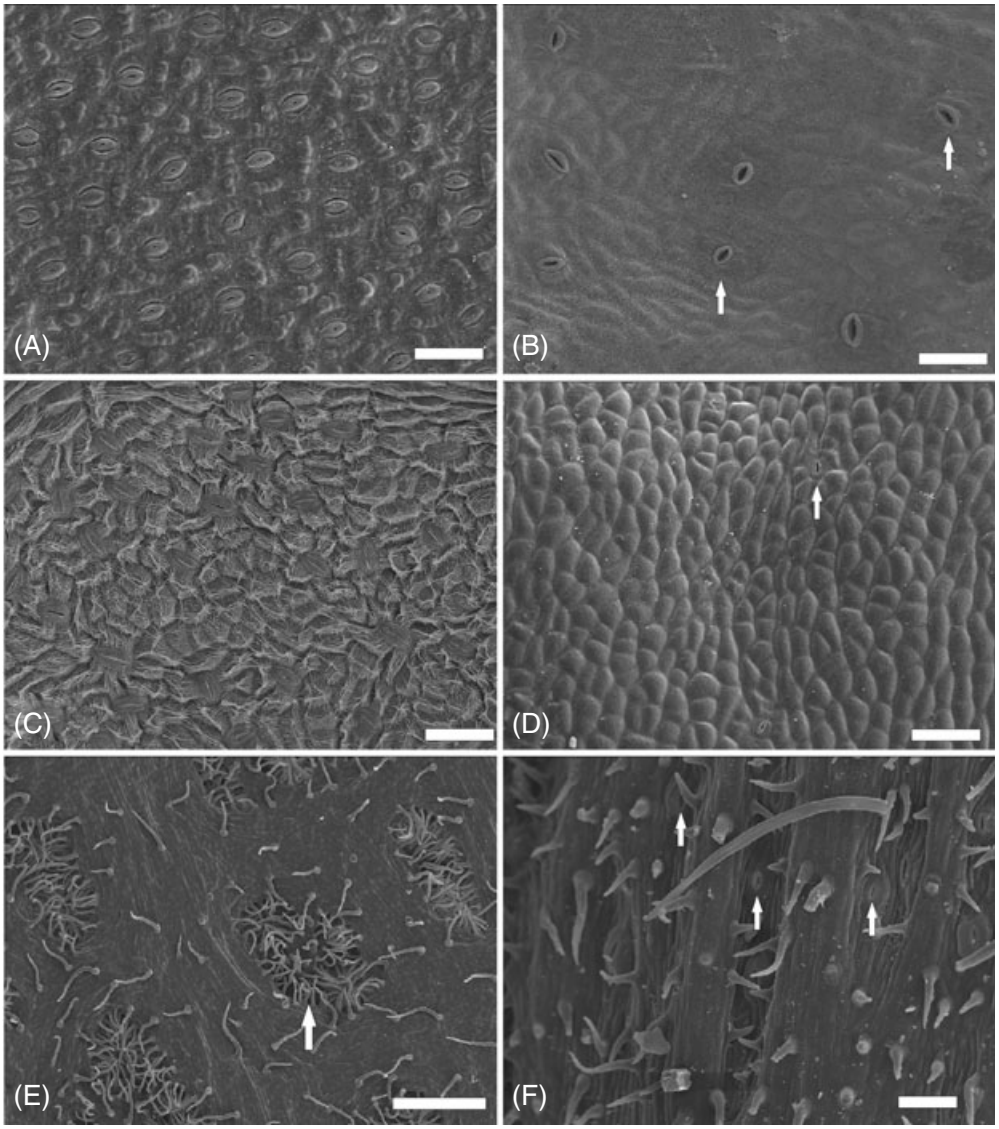

Fig. 1. SEM micrographs of leaf (left column) and pericarp (right column) surface. (A), (B): *Acacia cyanophylla*; (C), (D): *Ailanthus altissima*. Note the abundance of stomata on leaves and their scarcity on pericarps [(B), (D) arrows)]. (E), (F): *Nerium oleander*. Stomata are restricted only in crypts [(E), arrow]. On the contrary, stomata are evenly distributed on pericarp surface [(F), arrows]. In Figs A–D and F bars = 50 μm. In Fig. 1E bar = 200 μm.

Table 1. Stomatal densities on leaf and pericarp surfaces (number of stomata mm^{-2}). Data are means ± SD from 20 independent measurements. The superscript alphabets for each plant indicate statistically significant differences ($P < 0.05$) between leaves and pericarps. The number of stomata mm^{-2} in leaves of *N. oleander* cannot be counted as stomata are restricted in crypts. Note that *A. cyanophylla* has amphistomatous leaves with similar densities on the two sides

	Leaf	Pericarp
Acacia cyanophylla	219 ± 32^a	55 ± 19^b
Ailanthus altissima	219 ± 14^a	15 ± 7^b
Nerium oleander		44 ± 15

by one-way analysis of variance (ANOVA) (SPSS 15.00 statistical package). The number of independent measurements in each case is given in the legends of figures and tables.

Results and discussion

Fig. 1 shows SEM photographs of abaxial leaf and pericarp surfaces. Stomata on the leaf of *N. oleander* are not apparent as they are located in crypts. As expected, calculated stomatal densities are far less in the pericarps, as shown in Table 1. Accordingly,

Table 2. Pigment ratios (g g^{-1}) in leaves and fruits of the indicated species. Data are means ± SD from 10 (*Acacia cyanophylla, Ailanthus altissima*) and 20 (*Nerium oleander*) independent measurements. The superscript alphabets within each row and for each parameter indicate statistically significant differences ($P < 0.05$)

	Chl *a*/Chl *b*			Car/Chl		
	Leaf	Pericarp	Seed	Leaf	Pericarp	Seed
Acacia cyanophylla	2.68 ± 0.10^a	2.44 ± 0.13^b	2.04 ± 0.53^c	0.11 ± 0.02^a	0.14 ± 0.02^b	0.24 ± 0.04^c
Ailanthus altissima	2.64 ± 0.08^a	2.12 ± 0.16^b	–	0.13 ± 0.01^a	0.19 ± 0.03^b	–
Nerium oleander	3.38 ± 0.13^a	3.05 ± 0.20^b	3.11 ± 0.54^b	0.19 ± 0.01^a	0.26 ± 0.02^b	0.39 ± 0.09^c

we can reasonably assume that diffusive resistance of fruit epidermises in our test species is high, as observed with fruits of other species (Moreshet and Green 1980, Schotsmans et al. 2003, Wullschleger and Oosterhuis 1991). Hence, a hypoxic and CO_2-enriched internal atmosphere may be deduced (see Introduction section), although corresponding measurements were not performed in the present study.

Fruits had less chlorophyll than leaves. On a surface area basis, pericarps contained 19–34% of the leaf chlorophyll depending on species. On a dry mass basis, pericarps contained 12–19% and seeds 5–9% of the leaf chlorophyll. Pigment ratios are shown Table 2. Chl *a*/Chl *b* was consistently lower but Car/Chl was consistently higher in pericarps and seeds. A low Chl *a*/Chl *b* ratio is indicative of a shade adaptation because in shaded photosynthetic tissues light-harvesting antennas (containing both Chl *a* and Chl *b*) increase in size at the expense of reaction centers (containing only Chl *a*) (Anderson 1986). However, this may only explain the low Chl *a*/Chl *b* ratios in seeds which are effectively shaded by pericarps. It cannot explain the low Chl *a*/Chl *b* ratios in pericarps compared with leaves, as both leaves and fruits were sampled from equally exposed places. On the other hand, a high Car/Chl ratio may denote an increased need for harmless dissipation of extra excitation energy in fruits (Demmig-Adams et al. 1996). This will be discussed later in conjunction with correspondingly high yields of non-photochemical energy quenching in fruits.

When plotted on a logarithmic time scale, the kinetics of fluorescence rise displayed similar profiles, with distinct O-J-I-P steps in all cases. As an example, transients from *A. cyanophylla* are presented in Fig. 2, expressed as relative variable fluorescence, $V_t = (F_t - F_0)/(F_P - F_0)$, i.e. after double normalization at the F_0 and F_P steps. Despite profile similarity, the transient from pericarps lies higher than leaf and that from seeds is even higher, indicating that the fraction of closed PSII reaction centers at any time is higher in fruit parts. The same was true for the other two test plants. There are two characteristic differences deserving further discussion. First, the initial slope of the curve is progressively higher from leaf to seed, indicating a higher fractional rate of Q_A reduction, i.e. a higher energy flux from antenna to PSII reaction centers. This, in turn, could be the result of bigger antenna size. A big antenna size characterizes shade-adapted photosynthetic tissues (Anderson 1986) and could explain the steeper initial slope in seeds, yet steeper initial slope is also evident in pericarps. Please note that to avoid complexities imposed by their light history, leaves and fruits were sampled from fully exposed canopies. Accordingly, an explanation based on shade acclimation may be rejected, at least for the pericarps. Hence, we initially assume that the characteristic fluorescence transients indicate intrinsic photosynthetic attributes not linked to light levels or environmental stress.

Increased initial slope may also result from an elevated K-step which, when present, is hidden in the V_t curve as presented in Fig. 2. To clarify this point, the so-called W_t transient from F_0 to F_J, $W_t = V_{(t)}/V_J = (F_t - F_0)/(F_J - F_0)$, is presented in Fig. 3 (left vertical axis), together with the difference kinetics ΔW_t, i.e. the kinetics

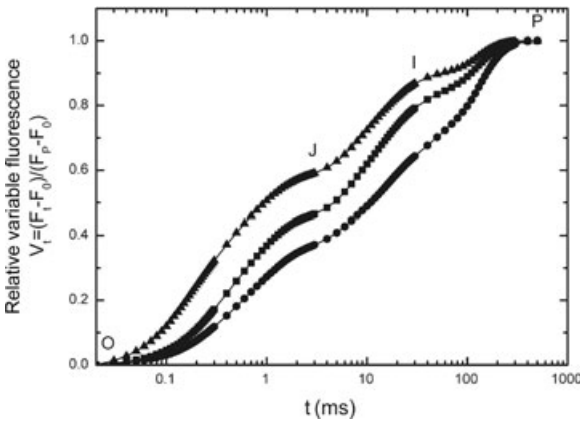

Fig. 2. Fast chlorophyll fluorescence transients (O-J-I-P) from leaves (circles), pericarps (squares) and seeds (triangles) of *Acacia cyanophylla* given on a logarithmic time scale and expressed as relative variable fluorescence (V_t), i.e. double normalized at the F_0 and F_P points. Each curve represents the mean of 20 independent transients.

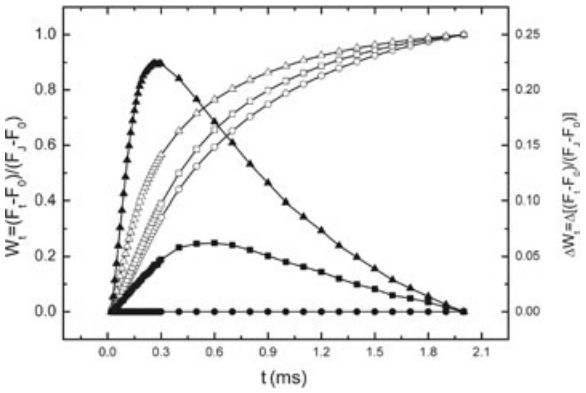

Fig. 3. W_t transients, i.e. double normalized at the F_0 and F_J points [left vertical axis, leaves (open circles), pericarps (open squares) and seeds (open triangles)], and ΔW_t transients, i.e. the double normalized kinetics for leaves, pericarps and seeds, after substraction of the leaf kinetics [right vertical axis, leaves (closed circles), pericarps (closed squares) and seeds (closed triangles)], from *Acacia cyanophylla*, given on a linear time scale. Each curve represents a mean of 20 independent transients.

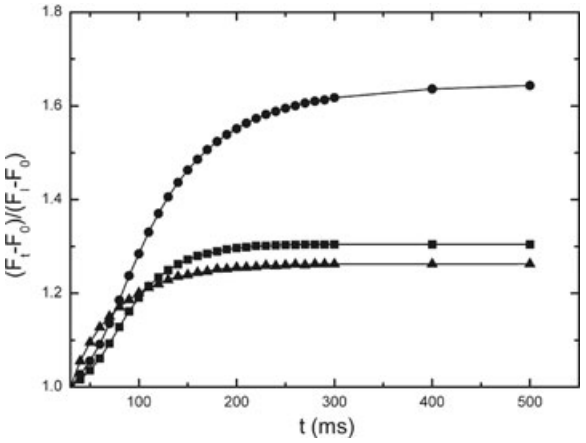

Fig. 4. Upper part of chlorophyll fluorescence transient from I to P, after double normalization between the F_0 and F_I points. Data from leaves (circles), pericarps (squares) and seeds (triangles) of *Nerium oleander* given on a linear time scale. Each curve represents the mean of 40 independent transients. Note that the starting point on the x-axis is 1 and the O-J-I part of the transient is omitted.

for pericarps and seeds, after substraction of the leaf kinetics (right vertical axis). Note that the time scale is linear. As shown, a distinct shoulder is evident at the K-band of the W_t curve (i.e. approximately 300–600 μs), especially in the seed. This is more clear in the ΔW_t kinetics displaying a strong peak at 300 μs for the seed and a broad peak at approximately 500–600 μs for the pericarp. Elevation of fluorescence yield at the K-band has been linked to a partial uncoupling of the oxygen evolving complex (OEC) (Srivastava et al. 1997), which may happen under environmental stress, especially heat stress. As such stress is not plausible at the period of sampling (late spring/early summer), we assume that the alleged partial uncoupling of OEC is an intrinsic character of fruit tissues.

A second point of concern is the considerable decrease in the relative amplitude of the I–P phase in fruits (see Fig. 2). There is experimental evidence that this phase is because of events in the vicinity of PSI, namely a bottle-neck of electron flow from PSI to the final electron acceptors, i.e. feredoxin and NADP (Schansker et al. 2005). Recently, a link between a low relative amplitude of the I–P phase and low PSI content was found (Oukarroum et al. 2009). A more clear picture of the I–P phase is given in Fig. 4, where the upper part of the $(F_t - F_0)/(F_I - F_0)$ transient is given in a linear time scale from t = 30 ms (I-step) to t = 500 ms (P-region). It has been proposed (Jiang et al. 2008, Tsimilli-Michael and Strasser 2008) that the I–P amplitude in the transient indicates the relative size of the pools of final PSI electron acceptors, which, according to Fig. 4, are smaller in fruits, especially in the seed.

From the curves of Fig. 4, the rate constants of reduction of the electron acceptor pools of PSI with electrons coming from the intersystem carriers can be calculated, as the time needed for the half saturation of these pools, i.e. $t_{1/2}{}^{(I-P)}$. Judging from Fig. 4, filling of PSI acceptors with electrons proceeds faster in pericarps and even faster in seeds. This is better shown graphically in Fig. 5, where the upper part (i.e. between 30 ms and 500 ms) of the relative variable fluorescence, double normalized at the I and P steps [i.e. $(F_t - F_I)/(F_P - F_I)$]

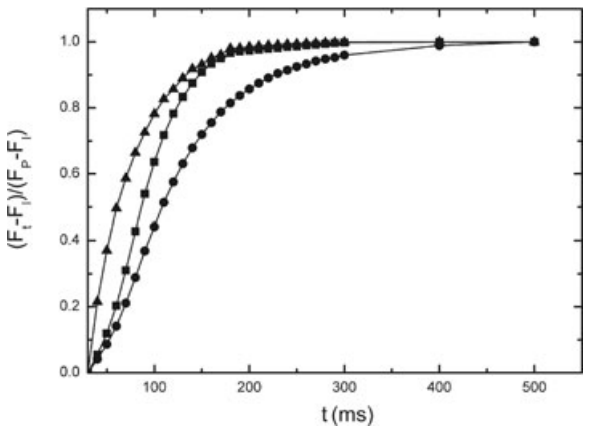

Fig. 5. Relative variable fluorescence transient from I to P, after double normalization between the F_I and F_P points. Data from leaves (circles), pericarps (squares) and seeds (triangles) of *Nerium oleander* given on a linear time scale. Each curve represents the mean of 40 independent transients.

Table 3. Numerical values for quantum yields and flux ratios (ϕ_{Po}, ϕ_{Do}, ϕ_{Eo}, ϕ_{Ro}, ψ_{Eo}, δ_{Ro}) and specific energy fluxes per Q_A-reducing PSII centers (ABS/RC, TR_0/RC, DI_0/RC) in leaves and fruits parts. Definitions and formulae are given in Materials and methods and Appendix sections. Moreover, the ratios V_K/V_J (as a relative measure of inactivation of OEC), $1/V_I = (F_M - F_0)/(F_I - F_0)$ (as a relative measure of the pool size of final electron acceptors of PSI) as well as the half rise time from F_I to F_P ($t_{1/2}^{(I-P)}$) are given. Values are means ± SD from 20 (*Acacia cyanophylla*, *Ailanthus altissima*) and 40 (*Nerium oleander*) independent measurements. The superscript alphabets for each parameter and each plant indicate significant differences ($P < 0.05$) between leaves, pericarps and seeds

	Acacia cyanophylla			*Ailanthus altissima*		*Nerium oleander*		
	Leaf	Pericarp	Seed	Leaf	Pericarp	Leaf	Pericarp	Seed
ϕ_{Po}	0.85 ± 0.01^a	0.82 ± 0.01^b	0.77 ± 0.03^c	0.84 ± 0.01^a	0.62 ± 0.05^b	0.80 ± 0.02^a	0.76 ± 0.07^b	0.78 ± 0.06^b
ϕ_{Do}	0.15 ± 0.01^a	0.18 ± 0.01^b	0.23 ± 0.03^c	0.16 ± 0.01^a	0.38 ± 0.05^b	0.20 ± 0.02^a	0.24 ± 0.07^b	0.22 ± 0.06^b
ϕ_{Eo}	0.57 ± 0.02^a	0.45 ± 0.01^b	0.32 ± 0.04^c	0.58 ± 0.03^a	0.23 ± 0.02^b	0.48 ± 0.06^a	0.31 ± 0.06^b	0.33 ± 0.05^b
ψ_{Eo}	0.68 ± 0.02^a	0.57 ± 0.02^b	0.44 ± 0.05^c	0.70 ± 0.03^a	0.43 ± 0.02^b	0.61 ± 0.07^a	0.44 ± 0.06^b	0.45 ± 0.07^b
ϕ_{Ro}	0.33 ± 0.04^a	0.18 ± 0.02^b	0.12 ± 0.04^c	0.24 ± 0.04^a	0.11 ± 0.01^b	0.30 ± 0.06^a	0.16 ± 0.03^b	0.13 ± 0.05^c
δ_{Ro}	0.58 ± 0.05^a	0.40 ± 0.04^b	0.37 ± 0.08^b	0.42 ± 0.06^a	0.47 ± 0.04^a	0.62 ± 0.08^a	0.52 ± 0.14^b	0.40 ± 0.14^c
V_K/V_J	0.32 ± 0.03^a	0.35 ± 0.02^a	0.50 ± 0.06^b	0.24 ± 0.02^a	0.87 ± 0.04^b	0.37 ± 0.05^a	0.53 ± 0.08^b	0.45 ± 0.13^c
$1/V_I$	1.64 ± 0.12^a	1.33 ± 0.13^b	1.11 ± 0.35^c	1.42 ± 0.09^a	1.21 ± 0.02^b	1.61 ± 0.19^a	1.28 ± 0.08^b	1.21 ± 0.13^c
$t_{1/2}^{(I-P)}$ (ms)	90 ± 14^a	80 ± 6^b	95 ± 27^a	107 ± 10^a	63 ± 8^b	81 ± 21^a	64 ± 13^b	36 ± 10^c
ABS/RC	1.48 ± 0.15^a	1.72 ± 0.10^b	2.57 ± 0.31^c	1.13 ± 0.10^a	5.66 ± 0.67^b	1.83 ± 0.30^a	2.85 ± 0.66^b	2.33 ± 0.81^c
TR/RC	1.26 ± 0.12^a	1.41 ± 0.08^b	1.98 ± 0.25^c	0.95 ± 0.07^a	3.47 ± 0.16^b	1.47 ± 0.21^a	2.13 ± 0.33^b	1.8 ± 0.52^c
DI_o/RC	0.22 ± 0.03^a	0.30 ± 0.02^b	0.59 ± 0.10^c	0.18 ± 0.02^a	2.19 ± 0.55^b	0.36 ± 0.09^a	0.73 ± 0.37^b	0.55 ± 0.35^c

is given on a linear time scale. Numerical values for $t_{1/2}^{(I-P)}$ for all cases are given in Table 3.

We tentatively conclude from the above qualitative approach that linear flow in fruit parts may be limited by an inherent uncoupling of the OEC and/or a relative lack of active PSII reaction centers, in the presence of a rather large antenna size. However, completion of electron flow toward the reducing side of PSI may be facilitated because of the low pools of PSI and its final electron acceptors and their high affinity for electrons. With this initial information, we proceed to the quantitative estimation of partial efficiencies for energy and electron flow according to the JIP-test (Strasser et al. 2004), including also a quantitative analysis of the IP phase (Jiang et al. 2008, Tsimilli-Michael and Strasser 2008, Zubek et al. 2009).

As shown in Table 3, the quantum yields of primary photochemistry (ϕ_{Po}), for electron transport to the intersystem carriers (ϕ_{Eo}) and for reduction of PSI end acceptors (ϕ_{Ro}) were lower in fruit tissues of all plants. The same was true for the probability that trapped excitation energy will be conserved as redox energy (ψ_{Eo}). Hence, we conclude that PSII in fruits suffers from considerable inactivation both in energy trapping and further electron flow. However, the probability of an electron from reduced intermediate carriers to reduce the end acceptor of PSI (δ_{Ro}) is lower in the fruits of the two test plants but not in the third (i.e *A. altissima*), indicating that a hindered electron flow along PSII does not necessarily mean a corresponding hindrance along PSI.

Table 3 also contains numerical manifestation of what we have already deduced from the qualitative assessment of the various curves in Figs 3–5, i.e. a partial uncoupling of OEC (as V_K/V_J), a lower content of PSI reaction centers (as $1 - V_I$), and their faster reduction (as $t_{1/2}^{(I-P)}$) in fruits of all tested plants. Noteworthy that the extreme apparent uncoupling of OEC in *A. altissima* pericarps is accompanied by the most extensive drops in quantum efficiencies for both energy trapping and electron flow along PSII. Finally, Table 3 shows also the parameters ABS/RC, TR_0/RC and DI_0/RC, i.e. the specific fluxes of absorbed, trapped and dissipated energy per active (i.e. Q_A-reducing) PSII centers. The parameter ABS/RC is a relative measure of antenna size feeding active PSII reaction centers (Strasser et al. 2004). As indicated, energy fluxes in fruits are higher for all plants.

Hence, the quantitative assessment confirmed the tentative conclusions from the qualitative differences of fast rise chlorophyll fluorescence transients. In short, linear electron flow in fruits is limited by intrinsic partial inactivation of both OEC and PSII. As relative antenna size (per Q_A-reducing PSII centers) is higher in fruits, a higher proportion of absorbed energy is dissipated as heat. However, some aspects of PSI function indirectly indicate facilitation in the transfer of reducing power to terminal acceptors. Given the above information, we asked whether the limitations observed in dark-adapted fruits (i.e. at time zero) would affect electron flow behavior in the light-adapted state. To that aim, the saturation pulse method was used to study the effects of actinic light of various irradiances on the yield of photochemical energy conversion.

Effective PSII yield (ϕ'_{Pt}) was lower in pericarps and even lower in seeds in all species and under all light levels tested. Results from *A. cyanophylla* are given in Fig. 6, while in Table 4 a summary of numerical values for all species at moderate and high PAR levels is presented. Corresponding values for ETR′ are normal for leaves, considerably lower in pericarps and extremely lower in seeds, where ETR′ at saturating PAR is just 2–8% of the values attained by leaves. These results are in agreement with previous reports (Borisjuk et al. 2005, De Lehmos Fihlo and Dos Santos Isaias 2004, Hetherington et al. 1998), yet the observed leaf/fruit differences are much more pronounced with the test plants of this investigation. Fruit tissues also tend to develop higher NPQ, especially at low PAR (Fig. 6 and Table 4). This may indicate an engagement of the xanthophylls cycle components and may be compatible with the higher Car/Chl ratios displayed by fruits (Table 2). Overall, a suppressed linear electron flow and a high need for non-photochemical energy dissipation are evident in fruits.

At this point, we may ask whether the observed photosystem attributes could decisively affect the gas composition of the internal atmosphere in fruits. Although light decreases internal CO_2 and increases O_2 in fruits, the levels of external atmosphere are not approached (Borisjuk et al. 2005). Hence, a function for internal gas homeostasis may be marginal, as it would need an unhindered linear electron flow and carbon reduction as an effective electron sink. Yet, both linear electron flow and CO_2 assimilation rates are considerably suppressed in fruits. Seeking for an additional significance for fruit photosynthesis, the apparent similarities in photosystem attributes between fruits and twigs cannot pass unnoticed. As in fruits (this investigation), trapping efficiency in twigs is lower than leaves (Filippou et al. 2007, Manetas and Pfanz 2005, Tausz et al. 2005) and this is not the result of sustained photoinhibition (Yiotis et al. 2009). Moreover, a high population of non-Q_b-reducing centers is evident in twigs (Kotakis et al. 2006) and the same can be deduced for fruits from the low probability for a trapped exciton to move an electron further than Q_A (Table 3). In both fruits and twigs, partial inactivation of PSII is accompanied by extremely low linear transport rates in the light-adapted state [Fig. 6B and Table 4; see also Borisjuk et al. (2005) and Hetherington et al. (1998) for other fruits, and Levizou and Manetas (2008) and Manetas (2004) for twigs]. However, the inability of PSII to act as an efficient electron donor to PSI and the reductive pentose phosphate cycle does not necessarily predispose to an equally inactive PSI. In fact, PSI in twigs was found to be engaged in active cyclic flow

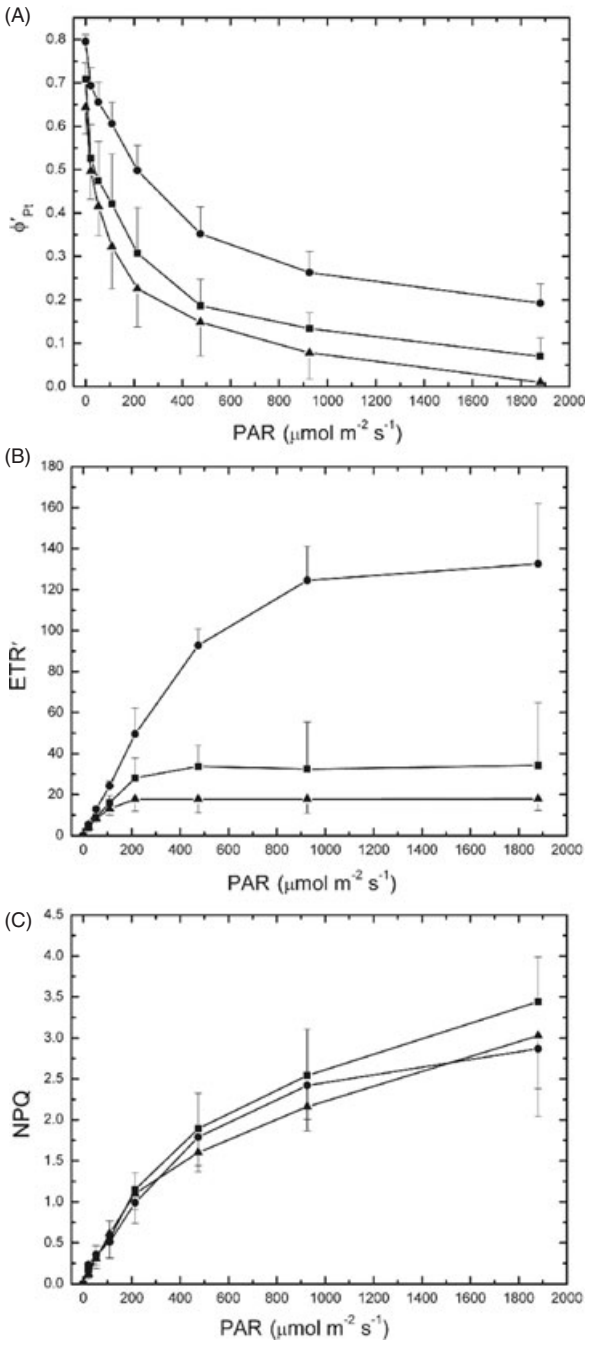

Fig. 6. Light dependence of PSII yield (ϕ'_{Pt}) and NPQ in leaves (circles), pericarps (squares) and seeds (triangles) of *Acacia cyanophylla*. Computed linear electron transport rates (ETR′) are also given. Data are means ± SD from 16 independent measurements.

(Ivanov et al. 2006, Kotakis et al. 2006). We argue that the same could be inferred for fruits, judging from the relative lack of sufficient end electron acceptors at PSI, which, if combined with the high rates of their reduction,

Table 4. Effective yield of PSII (ϕ'_{Pt}), linear electron transport rate (ETR′) and NPQ obtained at 200 and 1800 μmol m^{-2} s^{-1} PAR in leaves and fruits of the indicated species. Data are means ± SD from 16 (*Acacia cyanophylla* and *Ailanthus altissima*) and 32 (*Nerium oleander*) independent measurements. The superscript alphabets for each species and each parameter denote statistically significant differences ($P < 0.05$)

		ϕ'_{Pt}		ETR′		NPQ	
		200	1800	200	1800	200	1800
Acacia cyanophylla	Leaf	0.49 ± 0.05^{a}	0.19 ± 0.04^{a}	49.6 ± 12.6^{a}	132.6 ± 29.4^{a}	0.99 ± 0.20^{a}	2.86 ± 0.49^{a}
	Pericarp	0.31 ± 0.11^{b}	0.07 ± 0.04^{b}	28.1 ± 9.8^{b}	34.2 ± 30.7^{b}	1.14 ± 0.15^{b}	3.44 ± 0.54^{b}
	Seed	0.22 ± 0.08^{c}	0.01 ± 0.01^{c}	17.8 ± 5.8^{c}	17.9 ± 5.5^{c}	1.10 ± 0.20^{ab}	3.02 ± 0.98^{ab}
Ailanthus altissima	Leaf	0.55 ± 0.03^{a}	0.18 ± 0.03^{a}	47.3 ± 4.2^{a}	136.0 ± 25.1^{a}	0.86 ± 0.30^{a}	2.55 ± 0.55^{a}
	Pericarp	0.14 ± 0.03^{b}	0.03 ± 0.01^{b}	5.4 ± 3.2^{b}	10.6 ± 1.5^{b}	1.13 ± 0.53^{b}	3.31 ± 0.62^{b}
Nerium oleander	Leaf	0.48 ± 0.03^{a}	0.11 ± 0.02^{a}	39.6 ± 4.5^{a}	78.9 ± 18.4^{a}	0.77 ± 0.27^{a}	2.76 ± 0.58^{a}
	Pericarp	0.42 ± 0.06^{b}	0.07 ± 0.03^{b}	31.7 ± 5.2^{b}	51.3 ± 14.3^{b}	0.59 ± 0.27^{a}	2.72 ± 0.71^{a}
	Seed	0.09 ± 0.07^{c}	0.01 ± 0.01^{c}	2.6 ± 1.2^{c}	6.4 ± 5.2^{c}	1.41 ± 0.23^{b}	2.62 ± 0.29^{a}

could facilitate the diversion of electrons back to the intersystem carriers. In this case, the partial inactivation of PSII and the low linear electron flow activity would prevent strong reduction of plastoquinone.

We argue that a sufficient cyclic but deficient linear photosynthetic electron flow may be advantageous for organs such as stems and fruits under hypoxia. Under low partial O_2 pressures, oxidative phosphorylation in mitochondria is restricted (Geigenberger 2003) and ATP production reduced. Low ATP pools up-regulate glycolysis (Fernie et al. 2004) and hypoxia may also increase the expression of glycolytic at the expense of tricarboxylic acid (TCA) enzymes (Méchin et al. 2007), further reducing the ATP/NAD(P)H ratio. On the other hand, both linear and cyclic photosynthetic electron flows contribute to ATP production, but only linear flow results in Nicotinamide adenine dinucleotide phosphate (NADPH) production (Bukhov and Carpentier 2004, Johnson 2005). Accordingly, any suppression of the linear without concomitant suppression of the cyclic electron flow would increase the ATP/NADPH ratio, compromise for the ATP losses because of hypoxia and provide enough energy to sink organs with high metabolic activity such as fruits and stems. One may argue at this point that an efficient PSII activity would elevate internal oxygen level and restore mitochondrial phosphorylation activity, at least during the day. However, as Borisjuk and Rolletschek (2009) have recently pointed out, there are at least six arguments pointing to the importance of low internal oxygen in fruits for the smooth development of seeds.

In conclusion, we suggest that the similarities of photosynthetic electron flow attributes in fruits (this investigation) and twigs (Kotakis et al. 2006), i.e. in organs suffering from unavoidable hypoxia while maintaining a high metabolic activity, may not be a mere coincidence. A function for chloroplasts as valves for the adjustment of ATP/NADPH ratios is proposed instead.

References

Anderson JM (1986) Photoregulation of the composition, function, and structure of thylakoid membranes. Annu Rev Plant Physiol Plant Mol Biol 37: 93–136

Aschan G, Pfanz H (2003) Non-foliar photosynthesis – a strategy of additional carbon acquisition. Flora 198: 81–97

Aschan G, Pfanz H, Vodnik D, Batič F (2005) Photosynthetic performance of vegetative and reproductive structures of green hellebore (*Helleborus viridis* L. agg.). Photosynthetica 43: 55–64

Bazzaz FA, Carlson RW, Harper JL (1979) Contribution to reproductive effort by photosynthesis of flowers and fruits. Nature 279: 554–555

Blanke MM, Lenz F (1989) Fruit photosynthesis. Plant Cell Environ 12: 31–46

Borisjuk L, Nguyen TH, Neuberger T, Rutten T, Tschiersch H, Claus B, Feussner I, Webb AG, Jakob P, Weber H, Wobus U, Rolletschek H (2005) Gradients of lipid storage, photosynthesis and plastid differentiation in developing soybean seeds. New Phytol 167: 761–776

Borisjuk L, Rollentschek H (2009) The oxygen status of the developing seed. New Phytol 182: 17–30

Bukhov N, Carpentier R (2004) Alternative Photosystem I-driven electron transport routes: mechanisms and functions. Photosynth Res 82: 17–33

Butler WL (1978) Energy distribution in photochemical apparatus of photosynthesis. Annu Rev Plant Physiol Plant Mol Biol 29: 345–378

Cernusak LA, Marshall JD (2000) Photosynthetic refixation in branches of Western White Pine. Funct Ecol 14: 300–311

De Lemos Filho JP, Dos Santos Isaias RM (2004) Comparative stomatal conductance and chlorophyll *a* fluorescence in leaves vs. fruits of the cerado legume

tree, *Dalbergia miscolobium*. Braz J Plant Physiol 16: 89–93
Demmig-Adams B, Gilmor AM, Adams WW III (1996) In vivo functions of carotenoids in higher plants. FASEB J 10: 403–412
Dima E, Manetas Y, Psaras GK (2006) Chlorophyll distribution pattern in inner stem tissues: evidence from epifluorescence microscopy and reflectance measurements in 20 woody species. Trees Struct Funct 20: 515–521
Fernie AR, Carrari F, Sweetlove LJ (2004) Respiratory metabolism: glycolysis, the TCA cycle and mitochondrial electron transport. Curr Opin Plant Biol 7: 254–261
Filippou M, Fasseas C, Karabourniotis G (2007) Photosynthetic characteristics of olive tree (*Olea europaea*) bark. Tree Physiol 27: 977–984
Geigenberger P (2003) Response of plant metabolism to too little oxygen. Curr Opin Plant Biol 6: 247–256
Genty B, Briantais J-M, Baker NR (1989) The relationship between quantum yield of photosynthetic electron transport and quenching of chlorophyll fluorescence. Biochim Biophys Acta 990: 87–92
Goffman FD, Ruckle M, Ohlrogge J, Shachar-Hill Y (2004) Carbon dioxide concentrations are very high in developing oilseeds. Plant Physiol Biochem 42: 703–708
Hetherington S, Smillie RM, Davies WJ (1998) Photosynthetic activities of vegetative and fruiting tissues of tomato. J Exp Bot 49: 1173–1181
Ivanov AG, Krol M, Sveshnikov D, Malmberg G, Gardeström P, Hurry V, Öquist G, Huner NPA (2006) Characterization of the photosynthetic apparatus in cortical bark chlorenchyma of Scots pine. Planta 223: 1165–1177
Jiang HX, Chen LS, Zheng JG, Han S, Tang N, Smith BR (2008) Aluminum-induced effects on Photosystem II photochemistry in Citrus leaves assessed by the chlorophyll *a* fluorescence transient. Tree Physiol 28: 1863–1871
Johnson GN (2005) Cyclic electron transport in C3 plants: fact or artifact. J Exp Bot 56: 407–416
Kotakis C, Petropoulou Y, Stamatakis K, Yiotis C, Manetas Y (2006) Evidence for active cyclic electron flow in twig chlorenchyma in the presence of an extremely deficient linear electron transport activity. Planta 225: 245–253
Levizou E, Manetas Y (2008) Maximum and effective PSII yields in the cortex of the main stem of young *Prunus cerasus* trees: Effects of seasons and exposure. Trees Struct Funct 22: 159–164
Lichtenthaler HK, Wellburn AR (1983) Determinations of total carotenoids and chlorophylls *a* and *b* of leaf extracts in different solvents. Biochem Soc Trans 603: 591–592
Manetas Y (2004) Probing corticular photosynthesis through in vivo chlorophyll fluorescence measurements: evidence that high internal CO_2 levels suppress electron flow and increase the risk of photoinhibition. Physiol Plant 120: 509–517
Manetas Y, Pfanz H (2005) Spatial heterogeneity of light penetration through periderm and lenticels and concomitant patchy acclimation of corticular photosynthesis. Trees Struct Funct 19: 409–414
Méchin V, Thévenot C, Le Guilloux M, Prioul JL, Damerval C (2007) Developmental analysis of maize endosperm proteome suggests a pivotal role for pyruvate orthophosphate dikinase. Plant Physiol 143: 1203–1219
Moreshet S, Green GC (1980) Photosynthesis and diffusion conductance of the valencia orange fruit under field conditions. J Exp Bot 31: 15–27
Oukarroum A, Schansker G, Strasser RJ (2009) Drought stress effects on photosystem I content and photosystem II thermotolerance analyzed using Chl *a* fluorescence kinetics in barley varieties differing in their drought tolerance. Physiol Plant 137: 188–199
Paillotin G (1976) Movement of excitations in the photosynthetic domains of photosystem II. J Theor Biol 58: 237–252
Pfanz H, Aschan G, Langefeld-Heyser R, Wittman C, Loose M (2002) Ecology and ecophysiology of tree stems – corticular and wood photosynthesis. Naturwissenschaften 89: 147–162
Schansker G, Tóth SZ, Strasser RJ (2005) Methylviologen and dibromothymoquinone treatments of pea leaves reveal the role of photosystem I in the Chl *a* fluorescence rise OJIP. Biochim Biophys Acta 1706: 250–261
Schotsmans W, Verlinden BA, Lammertyn J, Nicolai BM (2003) Simultaneous measurement of oxygen and carbon dioxide diffusivity in pear fruit tissue. Postharvest Biol Technol 29: 155–166
Srivastava A, Guissé B, Greppin H, Strasser RJ (1997) Regulation of antenna structure and electron transport in Photosystem II of *Pisum sativum* under elevated temperature probed by the fast polyphasic chlorophyll *a* fluorescent transient: OKJIP. Biochim Biophys Acta 1320: 95–106
Strasser RJ, Tsimili-Michael M, Srivastava A (2004) Analysis of the chlorophyll *a* fluorescence transient. In: Papageorgiou GC, Govindjee (eds) Chlorophyll *a* Fluorescence. A Signature of Photosynthesis. Springer, Dordrecht, pp 321–362
Tausz M, Warren CR, Adams MA (2005) Is the bark of shining gum (*Eucalyptus nitens*) a sun or a shade leaf? Trees Struct Funct 19: 415–421
Tsimilli-Michael M, Strasser RJ (2008) In vivo assessment of stress impact on plant's vitality: applications in detecting and evaluating the beneficial role of

mycorrhization on host plants. In: Varma A (ed) Mycorrhiza 3, Springer, Berlin, Heidelberg, pp 679–703
Wellburn AR (1994) The spectral determination of chlorophylls *a* and *b*, as well as total carotenoids, using various solvents with spectrophotometers of different resolution. J Plant Physiol 144: 307–313
Wittman C, Aschan G, Pfanz H (2001) Leaf and twig photosynthesis of young beech (*Fagus sylvatica*) and aspen (*Populus tremula*) trees grown under different light intensity regimes. Basic Appl Ecol 2: 145–154
Wullschleger SD, Oosterhuis DM (1991) Photosynthesis, transpiration, and water use efficiency of cotton leaves and fruit. Photosynthetica 25: 505–515
Xu HL, Gauthier L, Desjardins Y, Gosselin A (1997) Photosynthesis in leaves, fruits, stem and petioles of greenhouse-grown tomato plants. Photosynthetica 33: 113–123
Yiotis C, Petropoulou Y, Manetas Y (2009) Photosynthesis in light-remote plant tissues: evidence for light-independent and steeply decreasing PSII efficiency along twig depth in four tree species. Photosynthetica 47: 223–231
Zubek S, Turnau K, Tsimilli-Michael M, Strasser RJ (2009) Response of endangered plant species to inoculation with arbuscular mycorrhizal fungi and soil bacteria. Mycorrhiza 19: 113–123

Appendix

Cardinal points in the kinetics of fast chlorophyll fluorescence rise and the formulae used for the calculation of biophysical parameters, according to the JIP test

F_0	$F_{20\ \mu s}$, fluorescence intensity at 20 μs, considered as the fluorescence intensity when all reaction centers (RC) are open
F_m	Maximal fluorescence intensity, considered as the fluorescence intensity when all RCs are closed
F_v	Variable fluorescence, $F_m - F_0$
$F_{J\ or\ I}$	Fluorescence intensity at 2 ms or 30 ms, respectively
M_0 or $(dV/dt0)_0$	$4(F_{300\ \mu s} - F_0)/(F_m - F_0)$, initial slope of the fluorescence transient
V_K	$(F_{300\ \mu s} - F_0)/(F_m - F_0)$, relative variable fluorescence at 300 μs
V_J	$(F_{2\ ms} - F_0)/(F_m - F_0)$, relative variable fluorescence at 2 ms
V_I	$(F_{30\ ms} - F_0)/(F_m - F_0)$, relative variable fluorescence at 30 ms
Quantum yields or flux ratios	
ϕ_{Po} or TR_0/ABS	$F_v/F_m = 1 - F_0/F_m$
ϕ_{Do} or DI_0/ABS	$1 - \phi_{Po} = F_0/F_m$
ϕ_{Eo} or ET_0/ABS	$\phi_{Po} \cdot \psi_{Eo} = 1 - F_J/F_m$
ϕ_{Ro}	$\phi_{Po} \cdot \psi_{Eo} \cdot \delta_{Ro} = 1 - F_I/F_m$
ψ_{Eo} or ET_0/TR_0	$1 - V_J = (F_m - F_J)/(F_m - F_0)$
δ_{Ro}	$(1 - V_I)/(1 - V_J) = (F_m - F_I)/(F_m - F_J)$
Specific energy fluxes per active (Q_A-reducing) PSII center	
ABS/RC	$(M_0/V_J) \cdot F_m/(F_m - F_0)$
TR_0/RC	M_0/V_J
DI_0/RC	$(M_0/V_J) \cdot (F_0/F_V)$

Edited by T.C. Vogelmann